



## 1 Direct Rotational Ground Motion

The full linear elastic seismic displacement wavefield can be separated into **3 translational** ( $u$ ), **3 rotational** ( $\Omega$ ) and **6 strain** ( $\epsilon$ ) degrees of freedom (DoF):

$$u + \delta u = u + \epsilon \delta x + \Omega \times \delta x \text{ with } \Omega = \frac{1}{2} \frac{d}{dt} \nabla \times u$$

ROMY (Rotational Motion in seismology) has 4 large-scale ring laser gyroscopes providing direct, multi-component observations of rotational ground motion (Fig.2). Combined with a broad-band seismometer (FUR), 6 DoF analysis is possible. Currently, 3 rings are operational providing 3 rotational component observations.

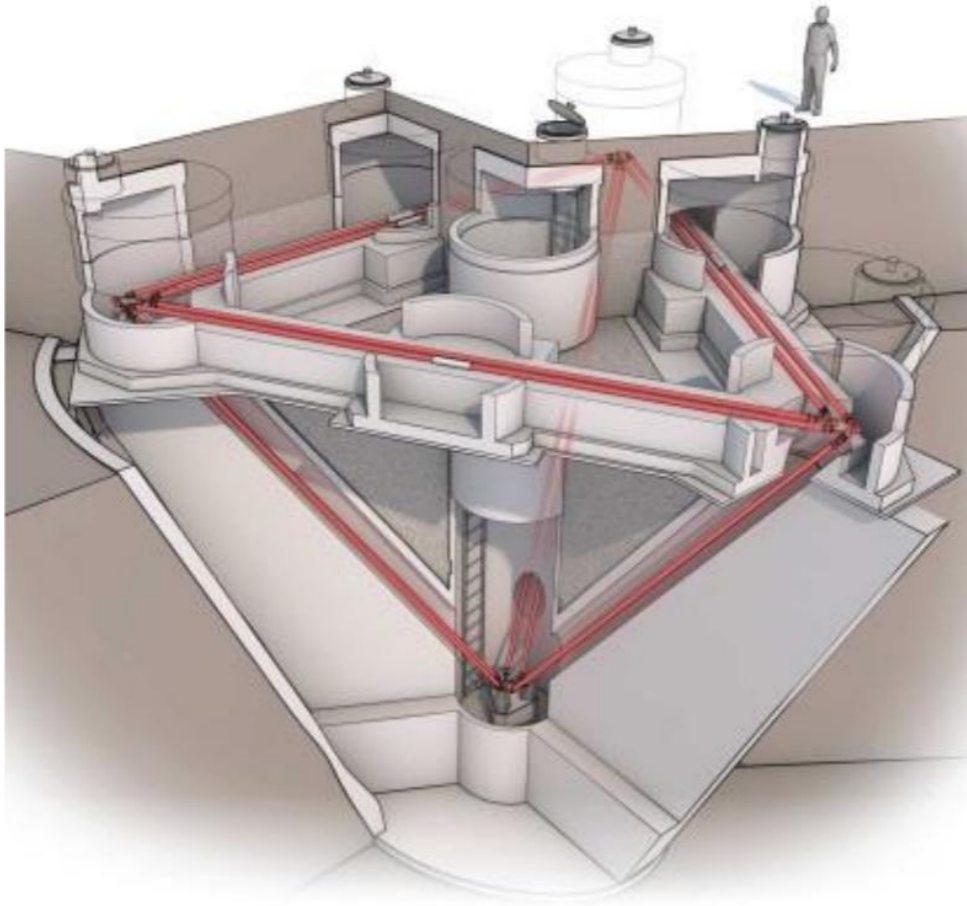


FIG 2: Schematic of ROMY's structure (Hand, 2017).

FIG 1: Translational ( $u$ ) and rotational ( $w$ ) ground motions.

## 2 Atmospheric Ground Deformation

Translational horizontal acceleration  $a_H$  records of inertial seismometers sense local rotation/tilt ( $\Omega$ ) that is dominantly caused by atmospheric loading:

$$a_H \approx g * \Omega = 9.81 \frac{m}{s^2} * \Omega$$

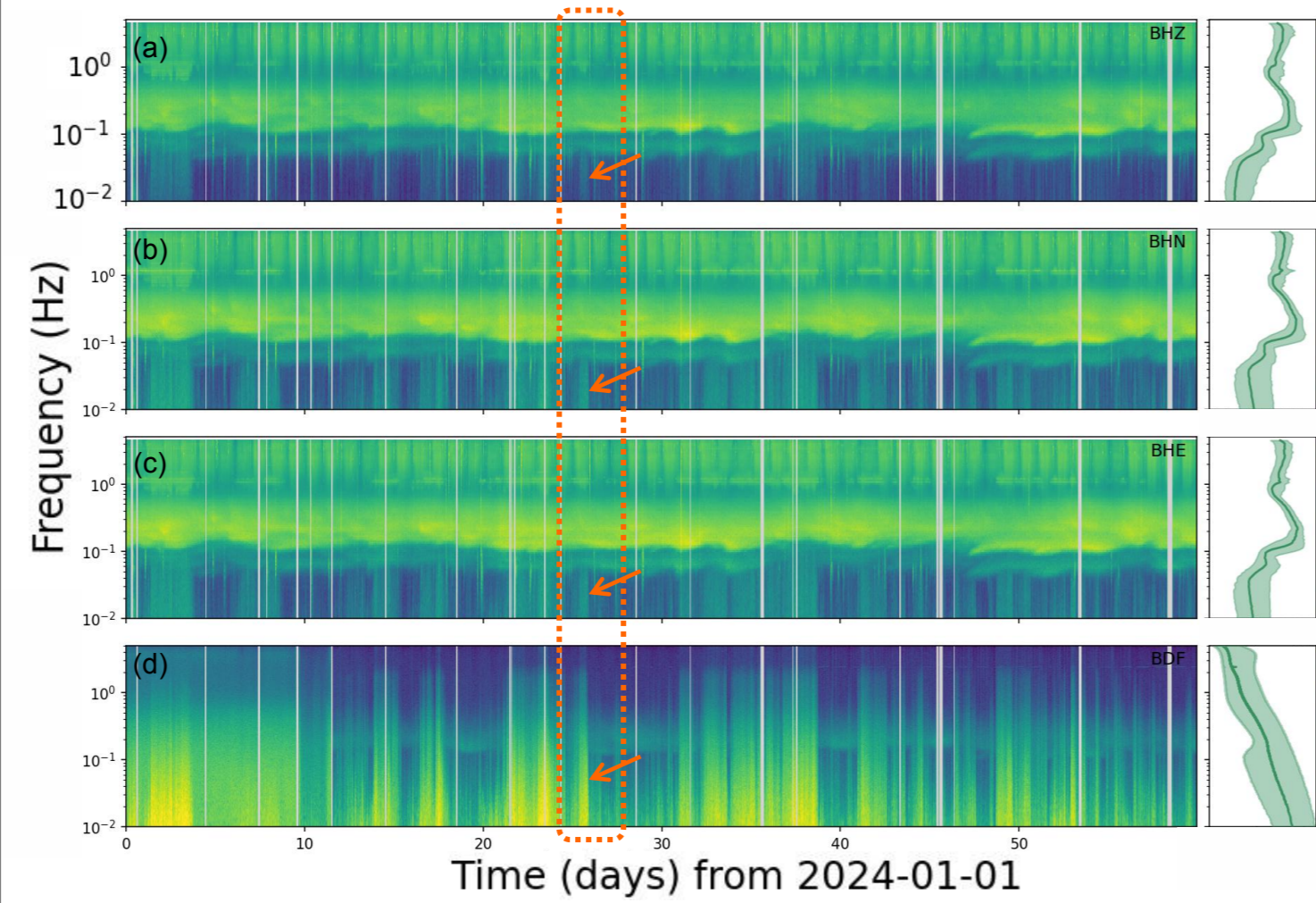
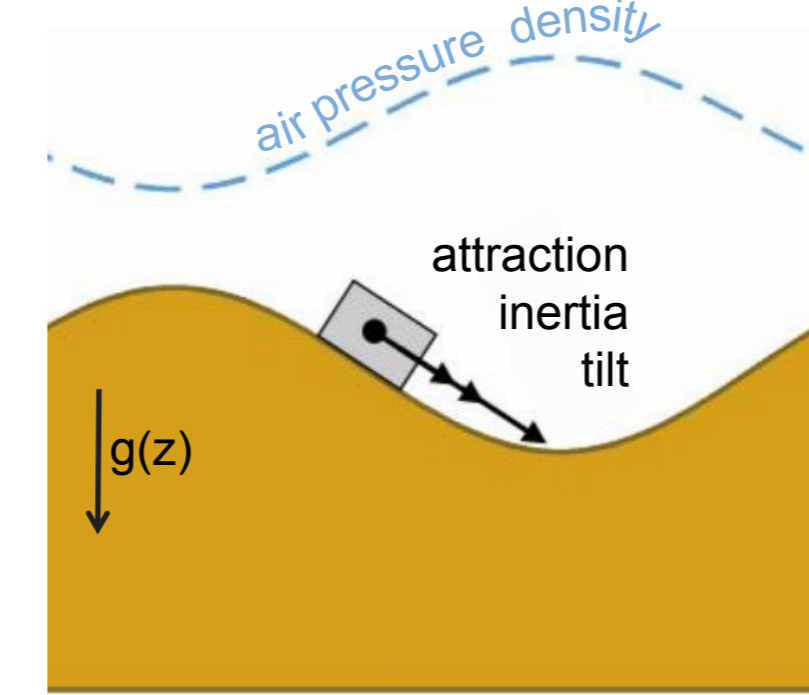


FIG 3: Spectrogram of acceleration (a-c) and co-located infrasound (d).

Energetic periods in infrasound (Fig. 3d) relate to elevated power levels for acceleration, especially for horizontal component records of FUR (Fig. 3a-c)

## 3 Deriving Admittance for Rotational Ground motions for Atmospheric Pressure

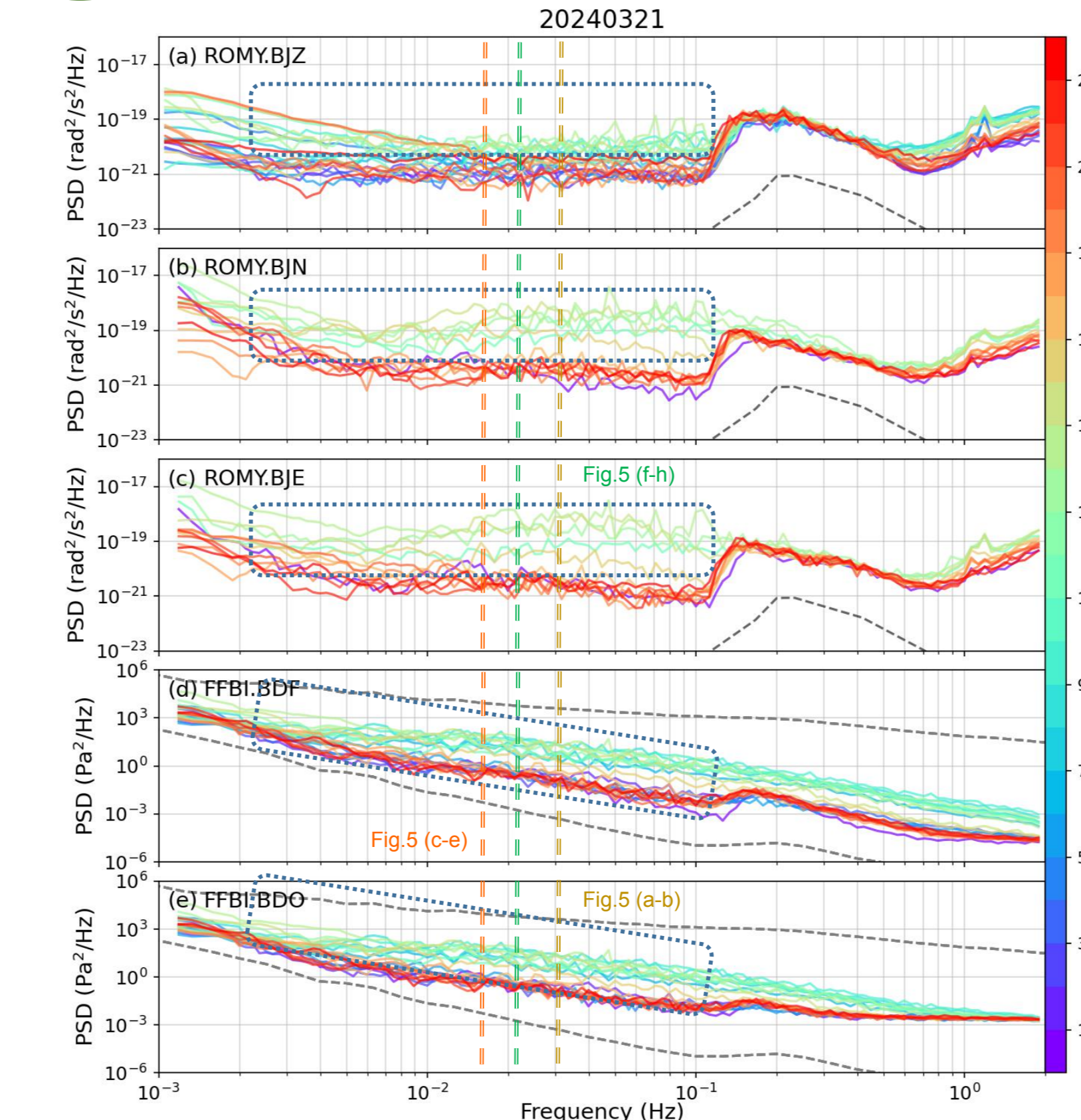


FIG 4: Hourly PSDs for rotation rate (ROMY) and pressure (FFBI) color-coded by hour-of-day.

- An increase in spectral power for atmospheric pressure between 07:00 and 17:00 on 2024-03-21 (Fig. 4) corresponds to an increase in rotation rate, in particular for horizontal rotations.
- A barometer (MB2005) provides infrasound (BDF) and absolute (BDO) atmospheric pressure observations (Fig. 4).
- Computing mean PSD and coherence values in 12<sup>th</sup>- octave frequency bands for several weeks reveals a pressure admittance for ground motions (Fig. 5).
- We estimate admittance using intercepts of a linear regression model for coherence values > 0.8 (red) and apply a constant offset (purple) as shown in Figure 5.

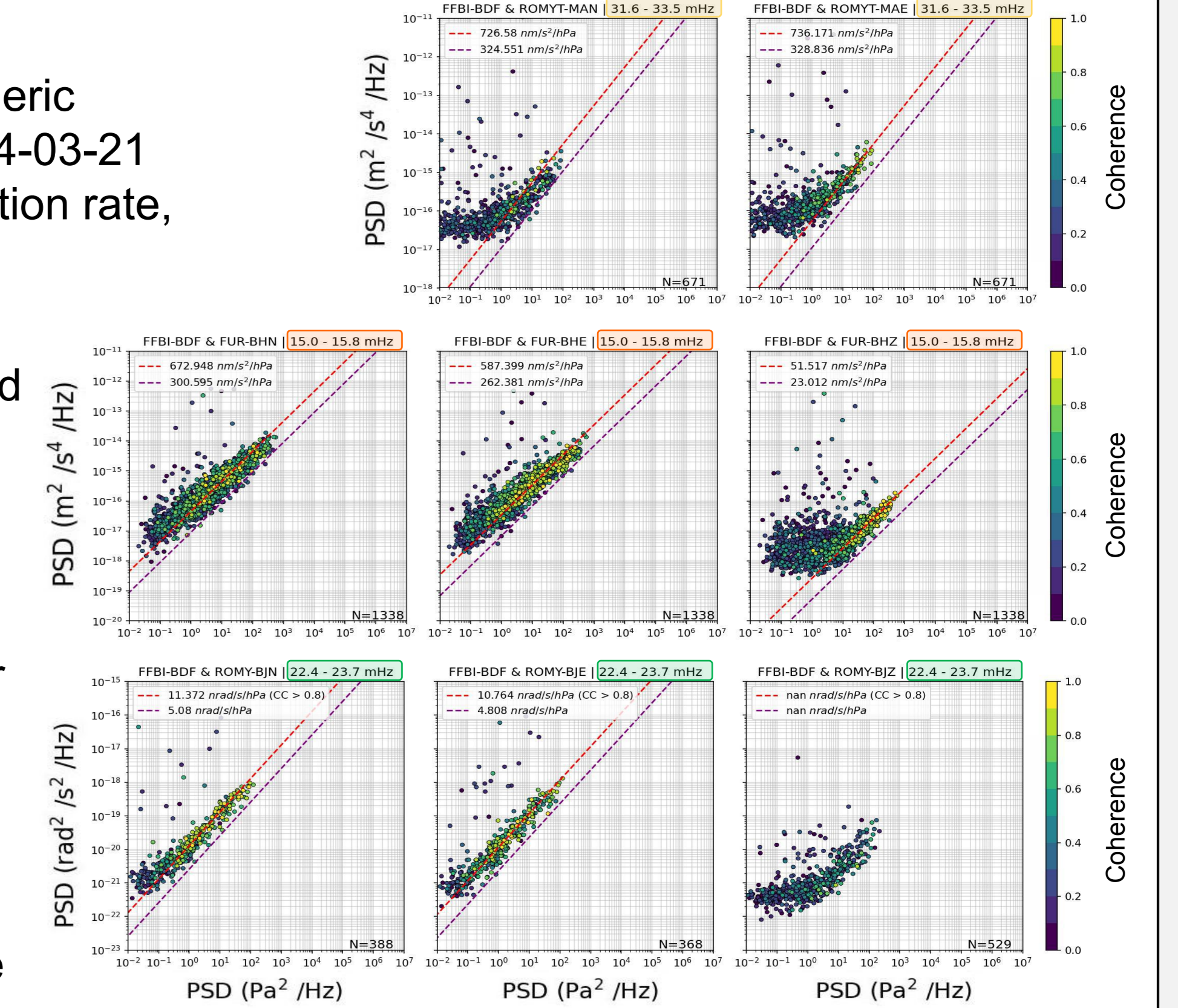


FIG 5: Mean PSD values of (a-b) tilt, (c-e) acceleration and (f-h) rotation rate components versus air pressure for exemplary frequency bands, color-coded by coherence.

## 4 Consequences for ROMY's Noise Model

We are interested to quantify and understand noise limitations for rotational ground motions at ROMY for low frequencies caused by atmospheric pressure coupling.

- Derived atmospheric pressure admittance for rotation rates at ROMY and RLAS (G-ring laser in Wettzell, Germany) and accelerations at BFO and FUR are shown in Figure 6a and 6b respectively. Median barometric pressure observed at ROMY is related to low and high noise models by Marty et al. (2021) in Figure 6c and 6d.
- By using the lower confidence limit of observed and the low noise model for barometric pressure levels and corresponding admittances, the expected level of minimum ground rotation rate can be estimated and compared to proposed low noise models for rotation rate (Brotzer et al. 2023) and translational acceleration (Petersen 1993).
- A different admittance and noise level for horizontal and vertical components is observed and expected.
- The difference between ROMY (sediments) and G-ring (hard rock) is most likely due to local geological setting.

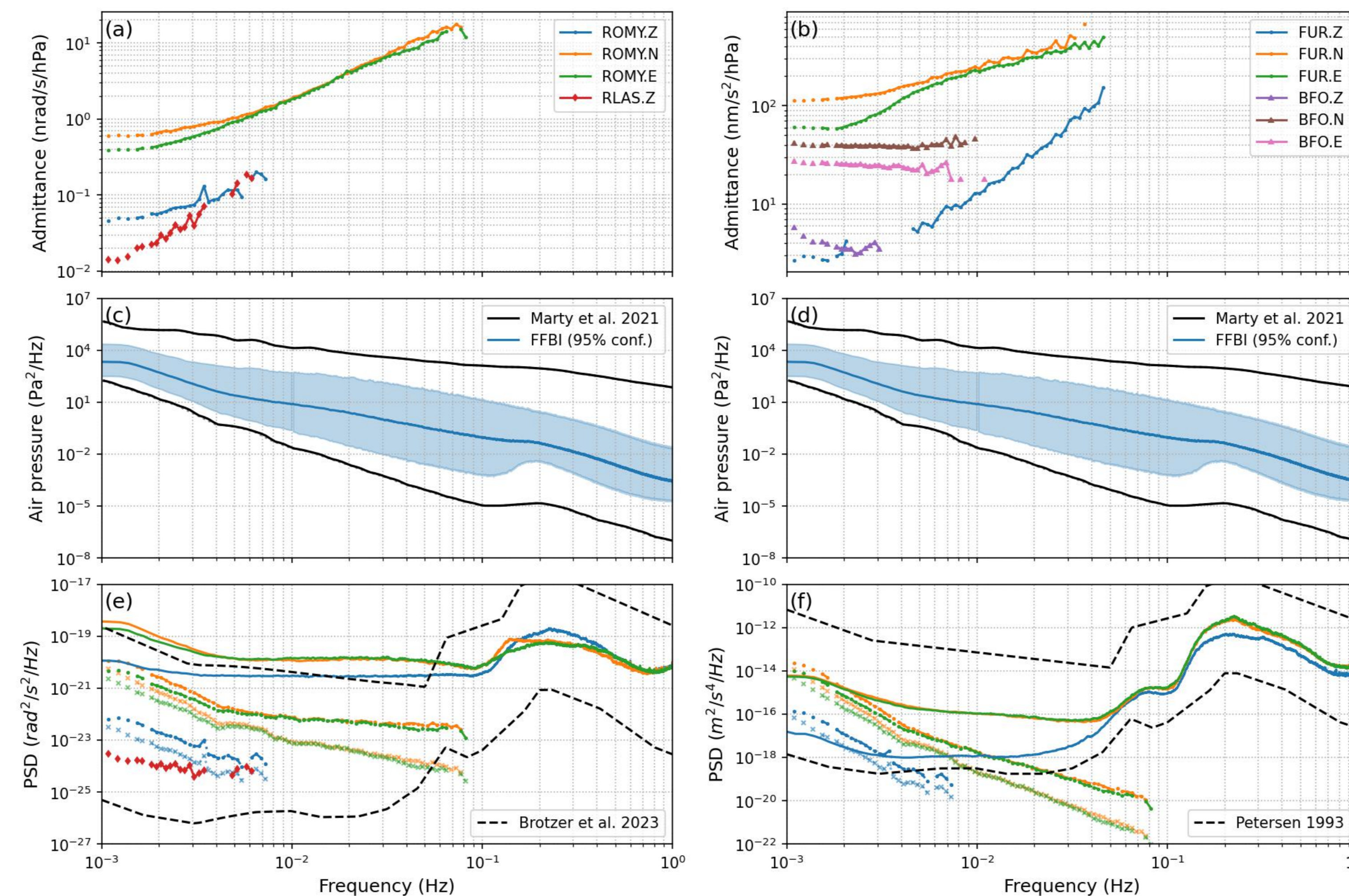


FIG 6: Admittance for rotation rate (a) and acceleration (b), observed pressure (FFBI) with low and high noise model (c,d) and minimum limits of rotation rate and acceleration by atmospheric coupling.

## 5 Conclusions and Outlook

- The noise level for horizontal and vertical rotation rate observations of ROMY for low frequencies is defined by local tilt deformation due to atmospheric pressure variation.
- High-quality direct observations of horizontal rotation might enable a correction for horizontal, low-frequency seismometer observations.
- Since March 2024, a small barometer array is operated around ROMY to observe local spatial pressure gradients. Figure 7 shows a snapshot of a passing atmospheric pressure field, which causes a transient load on the surface, causing local tilts.

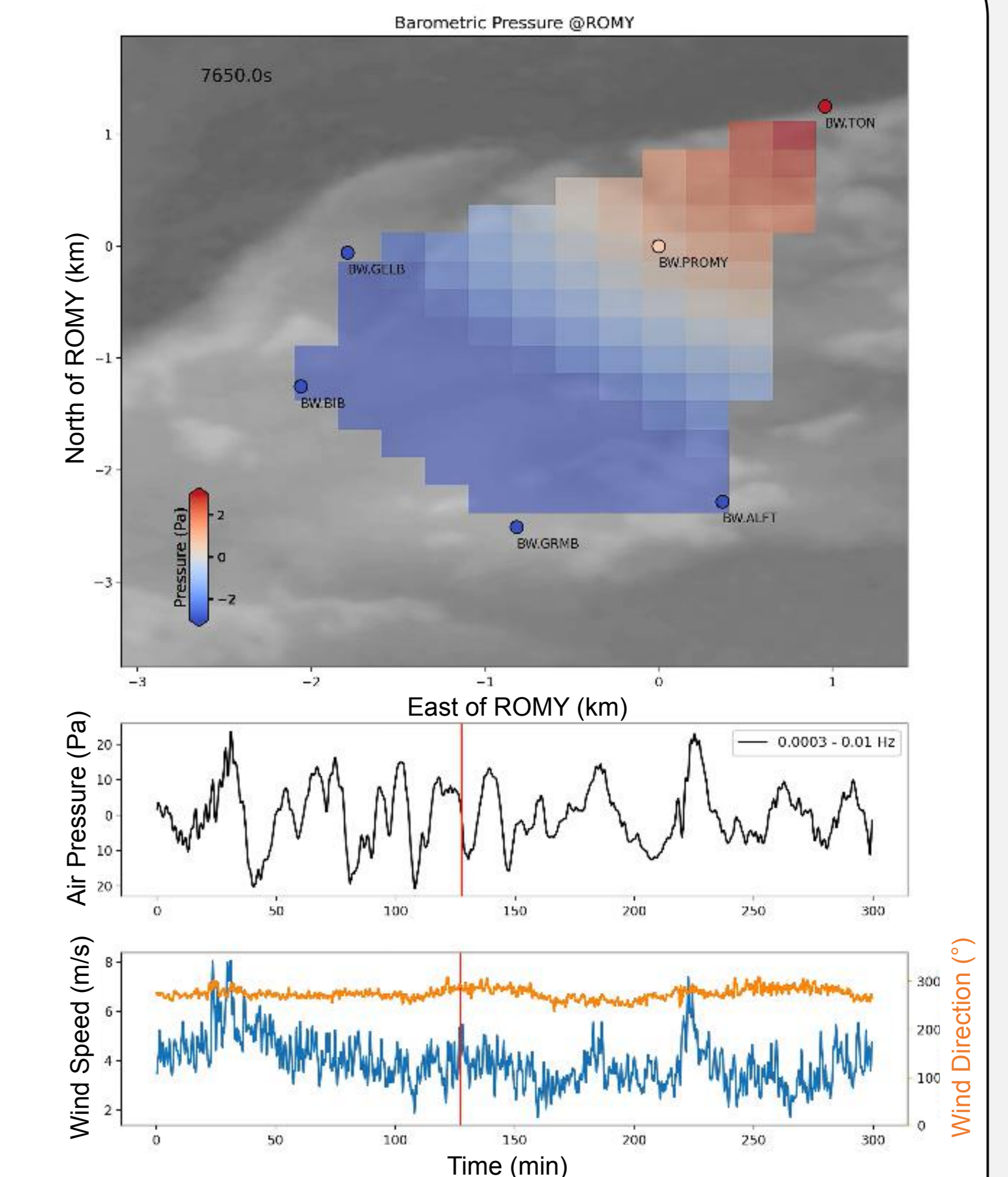


FIG 7: Snapshot of ROMY's barometer array to observe spatial barometric pressure gradients.

## Acknowledgments:

Our gratitude goes to the technical support team of ROMY.

## References:

- Hand (2017). Lord of the rings. Science. doi.org/10.1126/science.356.6335.23
- Marty et al. (2021). Low and high broadband spectral models of atmospheric pressure fluctuation. Journal of Atmospheric and Oceanic Technology. doi.org/10.1175/JTECH-D-21-0006.1
- Brotzer et al. (2023). Characterizing the Background Noise Level of Rotational Ground Motions on Earth. Seismological Research Letters. doi.org/10.1785/0220230202
- Petersen (1993). Observations and modeling of seismic background noise. USGS. doi.org/10.3133/ofr93322

## Contact

